Etch Rate Modeling in MEMS Design*†

Ted J. Hubbard
Department of Mechanical Engineering
Technical University of Nova Scotia
Halifax, Novia Scotia, Canada B3J 2X4
hubbardt@tuns.ca

Erik K. Antonsson‡
Engineering Design Research Laboratory
California Institute of Technology
Pasadena, California 91125-4400
erik@design.caltech.edu

April 24, 2000

Abstract

This paper presents a model for determining the full three dimensional etch rate behavior of bulk wet etching of silicon from experimentally determined etch rates of four principal planes: (100), (110), (111), and (311). The etch rate for an arbitrary plane is expressed in terms of the measured planes. The model shows excellent agreement with both experimental measurements and values reported in the literature. For MEMS CAD to be able to accurately predict etched shapes, a high quality 3D model of etch rates such as the one reported here is required.

Introduction

One common micro-machining technique is the anisotropic etching of silicon. Because the etching is anisotropic, the shape of an object changes with time. In order to model the time evolution of etched shapes, it is essential that the full etch rate diagram be well known. While some work has been done to characterize the full

*Manuscript prepared for submission to the *Journal of Modeling and Simulation of Microsystems*
†Word Count: 2470 words.
‡Corresponding author

three dimensional etch rate diagrams [2, 11, 13, 3, 7, 8, 14], more has been done to study the etch rates for a given wafer plane. Seidel, *et al*. [9] have studied the etch rate behavior of KOH in both the 100 and 110 planes. The 100 plane etch rate diagram has a characteristic four lobed rosette pattern while the 110 plane etch rate diagram is six-sided. The reasons for this behavior and other observed phenomena have not been fully examined. MEMS simulation systems such as the slowness method [10], ASEP [1], the Cellular Automata method [12, 6], the E-Shape method [4], and SEGS method [5] all require accurate etch rate data.

Unfortunately for most etchants only a few major planes are known, notably the (100), (110), (111) and perhaps the (311) planes. These planes are chosen because they tend to dominate most etched shapes, however they do not give the full picture. In this paper we will derive a model which supplies the full etch rate diagram given a few experimentally measured planes. The model requires a minimum of N planes to provide a N dimensional representation, but more planes may be utilized if they are available, providing a more accurate etch rate diagram. The model will first be derived for two dimensions with two parameters, then with three parameters. The same approach will be used for the three dimensional models with three and four parameters. The models show excellent agreement with both experimental measurements and values reported in the literature.

Two Dimensions

Consider a two dimensional vector $\{x, y\}$ defined by its Cartesian unit components $\hat{x}$ and $\hat{y}$ and its magnitude, or in polar coordinates, R and θ. The magnitude of the vector is the projection onto the wafer plane of a three dimensional etch rate. Because of silicon's symmetry, we need only look at 1/8th of the circle: $0 \leq \theta \leq \pi/4$ (or $0 \leq x \leq 1$ and $0 \leq y \leq x$). For example the (10), ($\bar{1}$0), and (01) vectors have the same rate since they belong to the (10) family. This use of symmetry simplifies the derivation, but the model is in no way limited to symmetrical systems. For asymmetrical systems all regions of the plane must be modeled.

Two Parameters

In two dimensions, two independent vectors are needed to define a basis. In the two parameter model there are two distinct rate vectors, the (10) vector at zero degrees and the (11) vector at 45 degrees. These vectors shall be called the principal vectors or principal rates.

These two dimensional rate vectors are the two dimensional projections of the three dimensional etch rates for different planes. The (11) vector is the projection

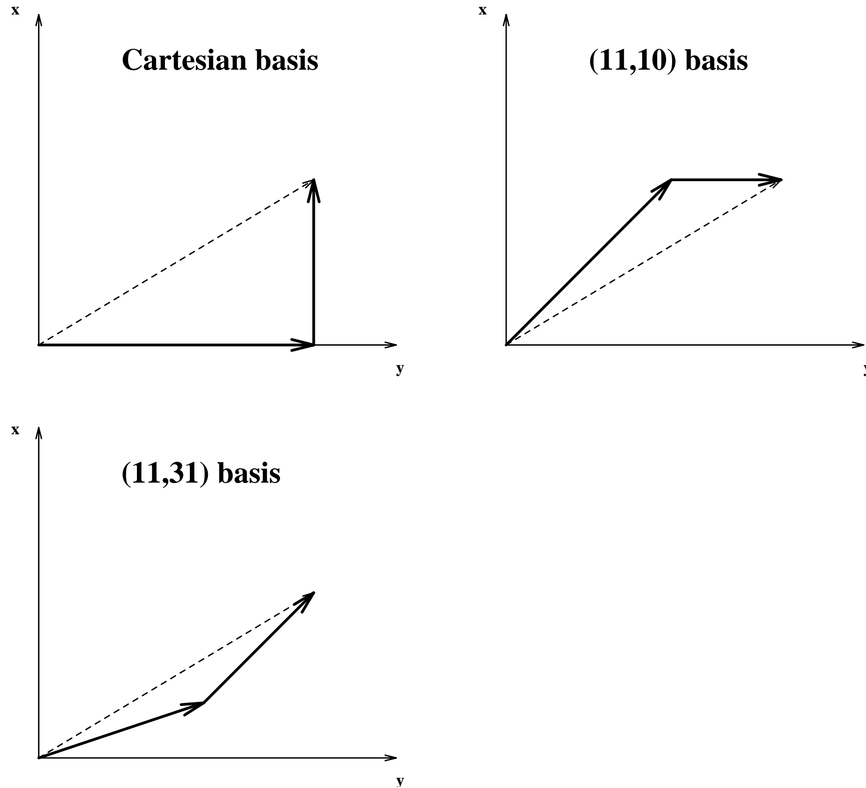

Figure 1: Two-Dimensional basis representations

of the (111) plane while the (10) vector is the projection of a (10$*$) plane, for example a (101) plane for EDP or a (100) plane for KOH.

In order to interpolate the etch rate of any arbitrary vector we wish to find its components not in terms of its Cartesian components but rather in terms of its (10) and (11) components. In other words we wish to transform from a representation in Cartesian space into a representation in the non-orthogonal basis of the two linearly independent principal rate vectors. We do this by multiplying the $\{\hat{x}, \hat{y}\}$ vector by the inverse of the basis matrix defined by the principal unit vectors. This is equivalent to solving two simultaneous equations to determine what magnitudes of the (10) and (11) vectors are required to construct an arbitrary vector. See Figure 1.

The condition that the interpolated rates be isotropic when the (10) and (11) rates are unity, is satisfied by using unit vectors. For example the (11) plane has unit Miller indices: $(1/\sqrt{2}, 1/\sqrt{2})$.

Every vector has a representation in the orthogonal Cartesian basis $\{x, y\}$. Let $\{a, b\}$ be the components of a unit vector $\{\hat{x}, \hat{y}\}$ in the non-orthogonal basis defined

basis	*equations*
$\begin{bmatrix} 1 & 0 \\ 1/\sqrt{2} & 1/\sqrt{2} \end{bmatrix}$	$a = \hat{x} - \hat{y}$ $b = \hat{y}/\sqrt{2}$

(3)

Table 1: 2D, Two parameter model matrices and equations

by the unit normals (unit Miller indices $\{\hat{h}, \hat{k}\}$) of two principal planes. Then:

$$\begin{bmatrix} a & b \end{bmatrix} = \begin{bmatrix} \hat{x} & \hat{y} \end{bmatrix} \begin{bmatrix} \hat{h}_1 & \hat{k}_1 \\ \hat{h}_2 & \hat{k}_2 \end{bmatrix}^{-1} \quad (1)$$

where ˆ signifies unit vectors. This relationship is valid within the triangular region defined by the two principal planes.

The etch rate at a vector $\hat{x}, \hat{y}$ is then given by a weighted sum of these components. By choosing the weights W_i to be the ratio of the ith rate to the (11) rate , it is possible to separate the shape of the etch rate diagram (ratio of rates) from the absolute size of the etch rate diagram ((11) rate). Thus $W_1 = 1$ and $W_2 = R_{(10)}/R_{(11)}$:

$$R(\hat{x}, \hat{y}) = (a * W_1 + b * W_2) * R_{11} \quad (2)$$

This formula is valid for all possible symmetric etchants: isotropic or highly anisotropic. Table 1 displays the details of this model. Note that the equations are only valid when a and b are positive, since the weights cannot be negative.

Because the (111) planes are the densest planes, they are usually the slowest. The ratio of the fastest to slowest planes ranges from 1 to 1 for the isotropic case to a few orders of magnitude for etchants such as KOH. For this reason it is not necessary to plot the etch rate diagrams for the cases where the ratio of (10) to (11) is less than unity, although the model would still be valid if small ratios etchants were available. Figure 2 show an array of such plots. Each element in the array has been scaled to fill an equal amount of space for display purposes. This has been done for all the arrays that follow.

Three Parameters

The effect of the (311) planes can be included by using a three parameter model. Again only the region $0 \leq \theta \leq \pi/4$ is considered, but there are now three principal rates (10), (11), and (31) where the (31) vector is the two dimensional projection of the (311) plane. The (10) and (11) rates appear in hole type shapes since they

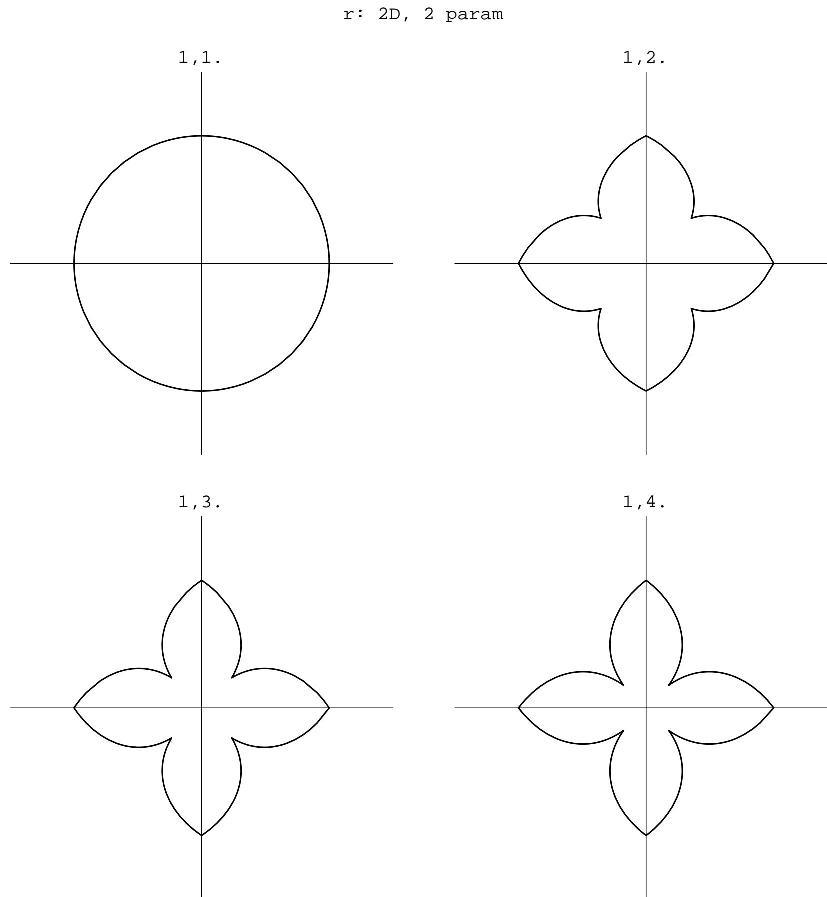

Figure 2: 2D, Two parameter results, the indices *e.g.* (1,2) represent the relative weight in the basis model of (11) and (10) planes

basis	*equations*
$\begin{bmatrix} 1 & 0 \\ 3/\sqrt{10} & 1/\sqrt{10} \end{bmatrix}$	$a = \hat{x} - 3\hat{y}$ $b = \sqrt{10}\hat{y}$
$\begin{bmatrix} 1/\sqrt{2} & 1/\sqrt{2} \\ 3/\sqrt{10} & 1/\sqrt{10} \end{bmatrix}$	$a = (-\hat{x}/2 + 3\hat{y}) * \sqrt{2}$ $b = \sqrt{10}/2(\hat{x} - \hat{y})$

(5)

Table 2: 2D, Three parameter model matrices and equations

are slow compared to faster planes such as the (31) rates. Pegs etched in EDP, KOH and similar etchants are bounded by eight (31) planes. Failure to include (31) rates will lead to peg type shapes that are bounded by four (10) planes. An N dimensional basis model requires a minimum of N parameters, however more parameters may be used. In order for the empirical fit to accurately model the etch rates, all extrema planes ((31) or otherwise) should be included. The (31) vector lies at about 18 degrees ($\arctan(1/3)$). Because only two vectors at a time may be used as a two dimensional basis, two regions are examined: $0 \leq \theta \leq \arctan(1/3)$ with (10) and (31) as the basis and $\arctan(1/3) \leq \theta \leq \pi/4$ with (31) and (11) as the basis. The derivation for the two parameter model is carried out again for the two regions producing two separate weighted sums each valid within its associated region. Note that the rates are continuous across the region interface. The net effect of the (31) rates is to produce secondary extrema. The results are rearranged to separate the size and shape effects as was done with the two parameter model. Furthermore by using the two parameter model we can find the default value for the (31)/(11) rate ratio required to collapse the three parameter model to two parameters:

$$\text{default } R_{31}/R_{11} = (1 + 2 * R_{10}/R_{11})/3 \tag{4}$$

Rearranging, we obtain a weighted sum in terms of R_{10}/R_{11}, the R_{31}/R_{11} default rate ratio, and the scaling factor by which the default is multiplied. Table 2 displays the details of this model. Note that the equations are only valid when a and b are positive, since the weights cannot be negative.

Again the availability of etchants is used to limit the R_{10}/R_{11} rates and the scaling factor to be larger than or equal to unity. Figure 3 show such plots.

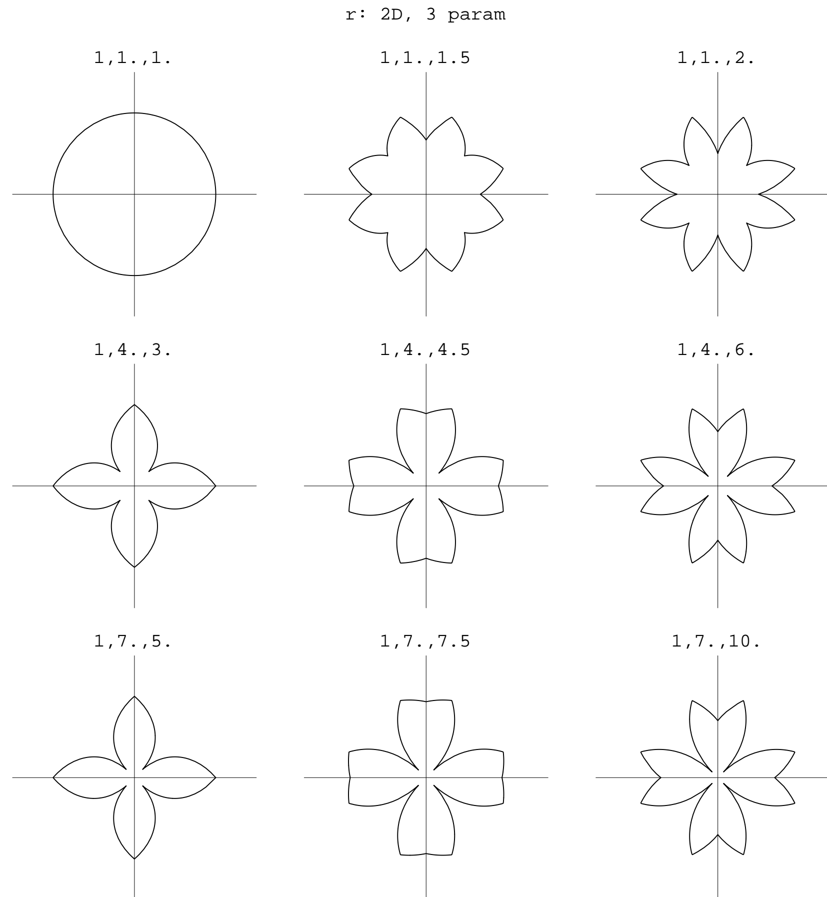

Figure 3: 2D, Three parameter results, the indices *e.g.* (1,4,3) represent the relative weight in the basis model of (11), (10), and (31) planes

Three Dimensions

Consider a vector $\{x, y, z\}$ in space defined by its Cartesian unit components $\hat{x}$, $\hat{y}$, and $\hat{z}$ and its magnitude, or in spherical coordinates R, θ, and ϕ. The magnitude of the vector is the three dimensional etch rate in the direction of the vector. Because of silicon's symmetry, we need only look at 1/16th of the sphere: $0 \leq \theta \leq \pi/4$ and $0 \leq \phi \leq \pi/2$ (or $0 \leq x \leq 1, 0 \leq y \leq x, 0 \leq z \leq 1$).

Three Parameters

In three dimensions, three independent vectors are needed to define a basis. The three principal vectors for the three parameter model are the (111), (100), and (110) rates. In this section of the sphere there are 5 principal planes in 3 families:

(100) family: (100) and (001)
(110) family: (110) and (101)
(111) family: (111)

From symmetry, all planes within a family have the same rate. The five planes form three triangular regions on the sphere each bounded by three basis vectors: (100,111,110), (100,111,101), and (001,111,101) as is shown in Figure 4.

For each triangular section, the representation of any arbitrary vector is found in the non-orthogonal basis by multiplying the vectors Cartesian components by the inverse of the 3 by 3 basis matrix. This is equivalent to solving three simultaneous equations to determine what magnitudes of the (100), (110), and (111) vectors are required to construct an arbitrary vector. The required rate is a weighted sum of the components expressed in terms of etch ratios.

Every vector has a representation in the orthogonal Cartesian basis x, y, z. Let $\{a, b, c\}$ be the components of a unit vector $\{\hat{x}, \hat{y}, \hat{z}\}$ in the non-orthogonal basis defined by the unit normals (unit Miller indices $\{\hat{h}, \hat{k}, \hat{l}\}$) of three principal planes. Then:

$$\begin{bmatrix} a & b & c \end{bmatrix} = \begin{bmatrix} \hat{x} & \hat{y} & \hat{z} \end{bmatrix} \begin{bmatrix} \hat{h}_1 & \hat{k}_1 & \hat{l}_1 \\ \hat{h}_2 & \hat{k}_2 & \hat{l}_2 \\ \hat{h}_3 & \hat{k}_3 & \hat{l}_3 \end{bmatrix}^{-1} \tag{6}$$

This relationship is valid within the triangular region defined by the three principal planes. The etch rate at a vector $\{\hat{x}, \hat{y}, \hat{z}\}$ is given by a weighted sum of these components:

$$R(\hat{x}, \hat{y}, \hat{z}) = (a * W_1 + b * W_2 + c * W_3) * R_{111} \tag{7}$$

where W_i is the relative etch rate or weight for the ith plane. Table 3 shows the details of this model. Again a, b, and c must be positive for the equations to be valid.

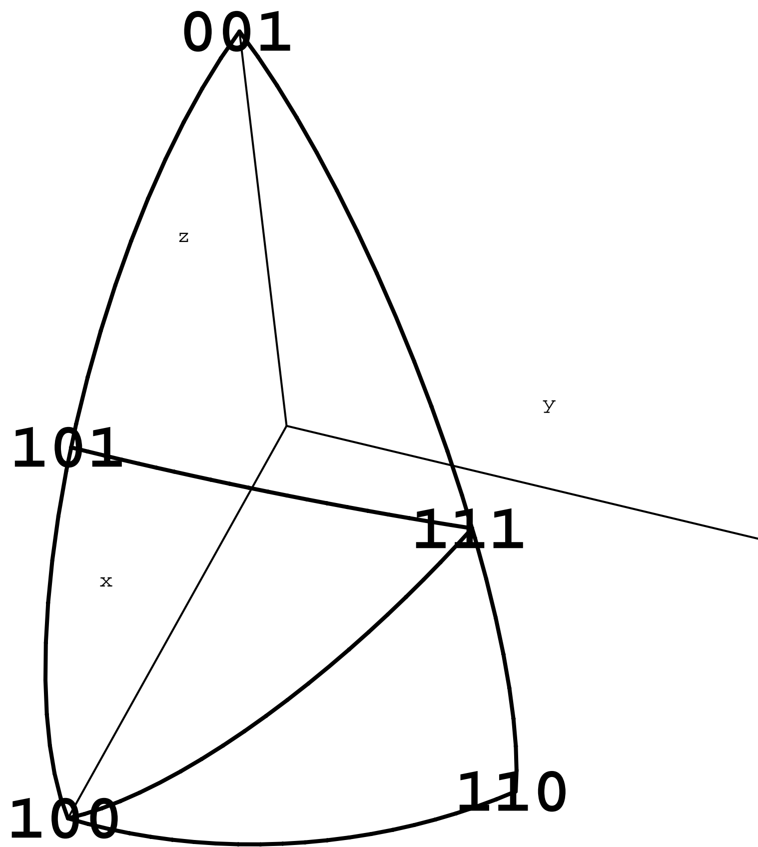

Figure 4: 3D, Three parameter model regions

$basis$	$equations$
$\begin{bmatrix} 1 & 0 & 0 \\ 1/\sqrt{2} & 1/\sqrt{2} & 0 \\ 1/\sqrt{3} & 1/\sqrt{3} & 1/\sqrt{3} \end{bmatrix}$	$a = \hat{x} - \hat{y}$ $b = \sqrt{2}(\hat{y} - \hat{z})$ $c = \hat{z}/\sqrt{3}$
$\begin{bmatrix} 1 & 0 & 0 \\ 1/\sqrt{2} & 0 & 1/\sqrt{2} \\ 1/\sqrt{3} & 1/\sqrt{3} & 1/\sqrt{3} \end{bmatrix}$	$a = \hat{x} - \hat{z}$ $b = \sqrt{2}(\hat{z} - \hat{y})$ $c = \sqrt{3}\hat{y}$
$\begin{bmatrix} 0 & 0 & 1 \\ 1/\sqrt{2} & 0 & 1/\sqrt{2} \\ 1/\sqrt{3} & 1/\sqrt{3} & 1/\sqrt{3} \end{bmatrix}$	$a = \hat{z} - \hat{x}$ $b = \sqrt{2}(\hat{x} - \hat{y})$ $c = \sqrt{3}\hat{y}$

(8)

Table 3: 3D, Three parameter model matrices and equations

This formula is valid for all possible symmetric etchants: isotropic or highly anisotropic. Figure 5 shows the etch rates for ratios greater than unity.

Four Parameters

The (311) rates are added to the model by redefining the triangular sections. In this case there seven vectors in the three principal families:

(100) family: (100) and (001)
(110) family: (110) and (101)
(111) family: (111)
(311) family: (113) and (311)

The new vectors require that the triangular sections be properly chosen. The seven planes form six triangular regions on the sphere each limited by three planes: (100,311,110), (100,101,311), (110,111,311), (101,111,311), (101,113,111), and (001,113,101) as is shown in Figure 6.

The etch rate at a vector $\{\hat{x}, \hat{y}, \hat{z}\}$ is given by a weighted sum of these components. Table 4 shows the details of this model. Figure 7 shows the etch rates for ratios greater than unity.

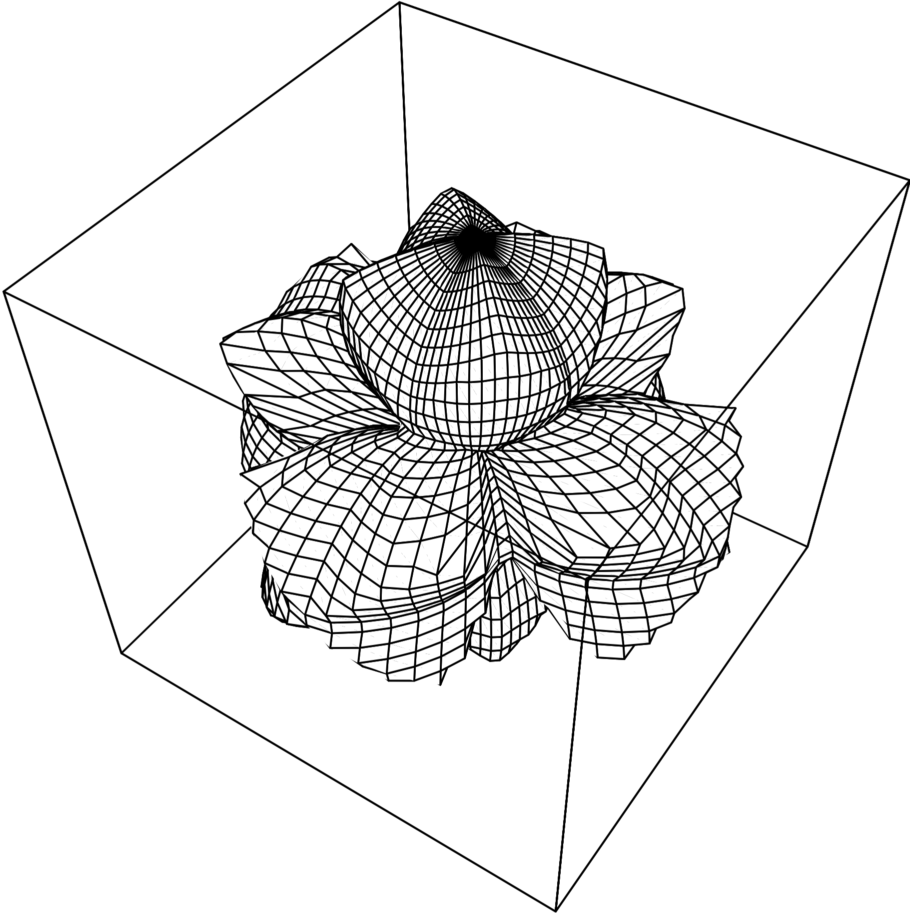

Figure 5: 3D, Three parameter model results

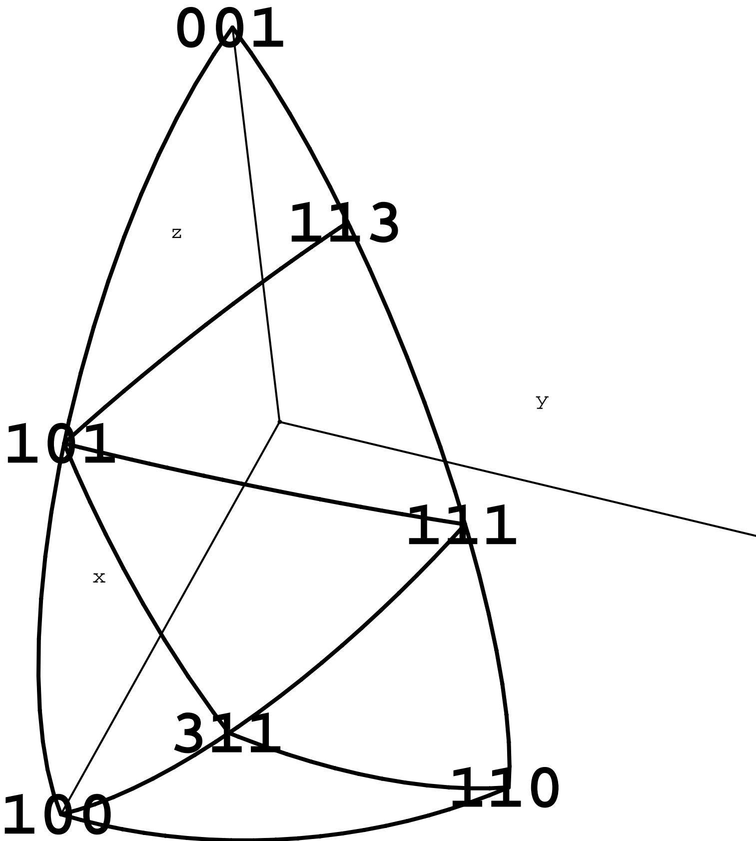

Figure 6: 3D, Four parameter model regions

$basis$	$equations$
$\begin{bmatrix} 1 & 0 & 0 \\ 1/\sqrt{2} & 1/\sqrt{2} & 0 \\ 3\sqrt{11} & 1\sqrt{11} & 1\sqrt{11} \end{bmatrix}$	$a = \hat{x} - \hat{y} - 2\hat{z}$ $b = \sqrt{2}(\hat{y} - \hat{z})$ $c = \sqrt{11}\hat{z}$
$\begin{bmatrix} 1 & 0 & 0 \\ 1/\sqrt{2} & 0 & 1/\sqrt{2} \\ 3/\sqrt{11} & 1/\sqrt{11} & 1/\sqrt{11} \end{bmatrix}$	$a = \hat{x} - 2\hat{y} - \hat{z}$ $b = \sqrt{2}(-\hat{y} + \hat{z})$ $c = \sqrt{11}\hat{y}$
$\begin{bmatrix} 1/\sqrt{3} & 1/\sqrt{3} & 1/\sqrt{3} \\ 1/\sqrt{2} & 1/\sqrt{2} & 0 \\ 3/\sqrt{11} & 1/\sqrt{11} & 1/\sqrt{11} \end{bmatrix}$	$a = \sqrt{3}/2(-\hat{x} + \hat{y} + 2\hat{z})$ $b = \sqrt{2}(\hat{y} - \hat{z})$ $c = \sqrt{11}/2(\hat{x} - \hat{y})$
$\begin{bmatrix} 1/\sqrt{3} & 1/\sqrt{3} & 1/\sqrt{3} \\ 1/\sqrt{2} & 0 & 1/\sqrt{2} \\ 3/\sqrt{11} & 1/\sqrt{11} & 1/\sqrt{11} \end{bmatrix}$	$a = \sqrt{3}/2(-\hat{x} + 2\hat{y} + \hat{z})$ $b = \sqrt{2}(-\hat{y} + \hat{z})$ $c = \sqrt{11}/2(\hat{x} - \hat{z})$
$\begin{bmatrix} 1/\sqrt{3} & 1/\sqrt{3} & 1/\sqrt{3} \\ 1/\sqrt{2} & 0 & 1/\sqrt{2} \\ 1/\sqrt{11} & 1/\sqrt{11} & 3/\sqrt{11} \end{bmatrix}$	$a = \sqrt{3}/2(\hat{x} + 2\hat{y} - \hat{z})$ $b = \sqrt{2}(\hat{x} - \hat{y})$ $c = \sqrt{11}/2(-\hat{x} + \hat{z})$
$\begin{bmatrix} 0 & 0 & 1 \\ 1/\sqrt{2} & 0 & 1/\sqrt{2} \\ 1/\sqrt{11} & 1/\sqrt{11} & 3/\sqrt{11} \end{bmatrix}$	$a = -\hat{x} - 2\hat{y} + \hat{z}$ $b = \sqrt{2}(\hat{x} - \hat{y})$ $c = \sqrt{11}\hat{y}$

(9)

Table 4: 3D, Four parameter model matrices and equations

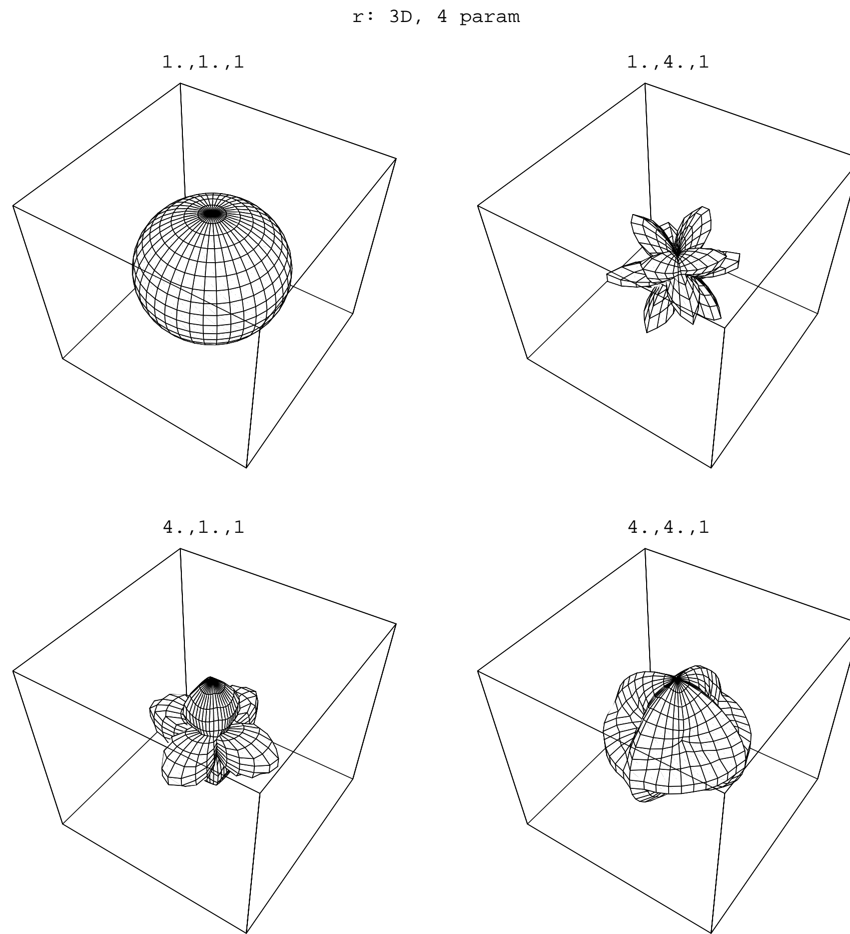

Figure 7: 3D, Four parameter model results, indices *e.g.* (4,1,1) represent the relative weight in the basis model of (110), (100), and (311) planes, and the (111) plane is given weight 1.0

2D (100) Projections of the 3D Model

When etched shapes are produced, the three dimensional etch rate diagrams are transformed into two dimensional etch rate diagrams projected onto the plane of the wafer cut. At each θ value in the plane a minimization in ϕ is performed to find the minimum projection onto the plane. For a (100) wafer this is:

$$\begin{aligned} R_{2d}(\theta) = MIN_{\phi}[proj(\theta, \phi)] \quad \Rightarrow \\ proj(\theta, \phi) = R_{3d}(\theta, \phi)/\cos(\phi - 90) \end{aligned} \tag{10}$$

Figure 8 shows such a minimization performed graphically.

The plane of the wafer corresponds to a maximum ϕ of 90 degrees. It is possible to perform this minimization for other maximum ϕ values, in this case the projection is onto a cone, as shown in Figure 9.

Three maximum ϕ values were examined, 90 degrees (the plane of wafer), 60, and 30 degrees. The maximum $\phi = 90°$ corresponds to the surface etch rate while the maximum $\phi = 60°$ and $30°$ give information about the etch rate deeper into the crystal. Thus there are three contours to plot the etch rate behavior. Closely packed contours indicate sharply sloped walls while widely spaced contours indicate walls with smaller slopes. Note that each contour represents constant ϕ and not constant depth. Figure 10 shows a modeled (100) projection while Figure 11 shows experimental data.

General Projections

This projection need not be limited to the (100) plane. In order to examine another plane the spherical coordinates in the new reference frame defined by the new wafer cut must be converted into the spherical coordinates in the (100) reference frame. If the old frame (ϕ, θ) is rotated by $\Delta\phi$ and $\Delta\phi$, the equations giving the new coordinates (ϕ_2, θ_2) are:

$$\cos(\phi_2) = \cos(\phi_2)\cos(\phi) - \cos(\theta)\sin(\Delta\phi)\sin(\phi) \tag{11}$$

$$\begin{aligned} \cos(\theta_2)\sin(\phi_2) \quad = \quad & \cos(\Delta\theta)\cos(\phi)\sin(\Delta\phi) \\ & + \cos(\Delta\phi)\cos(\Delta\theta)\cos(\theta)\sin(\phi) \\ & - \sin(\Delta\theta)\sin(\phi)\sin(\theta) \end{aligned} \tag{12}$$

where (ϕ_2, θ_2) defines the original frame.

For the (110) wafer $\Delta\theta = \pi/4$ and $\Delta\phi = 0$, while for the (111) wafer $\Delta\theta = \pi/4$ and $\Delta\phi = \pi/4$. The minimization is performed as before but the rate values used are those obtained from the new ϕ and θ. Figure 12 shows such a (110) projection; reported (110) projections are in excellent agreement as shown in Figure 13.

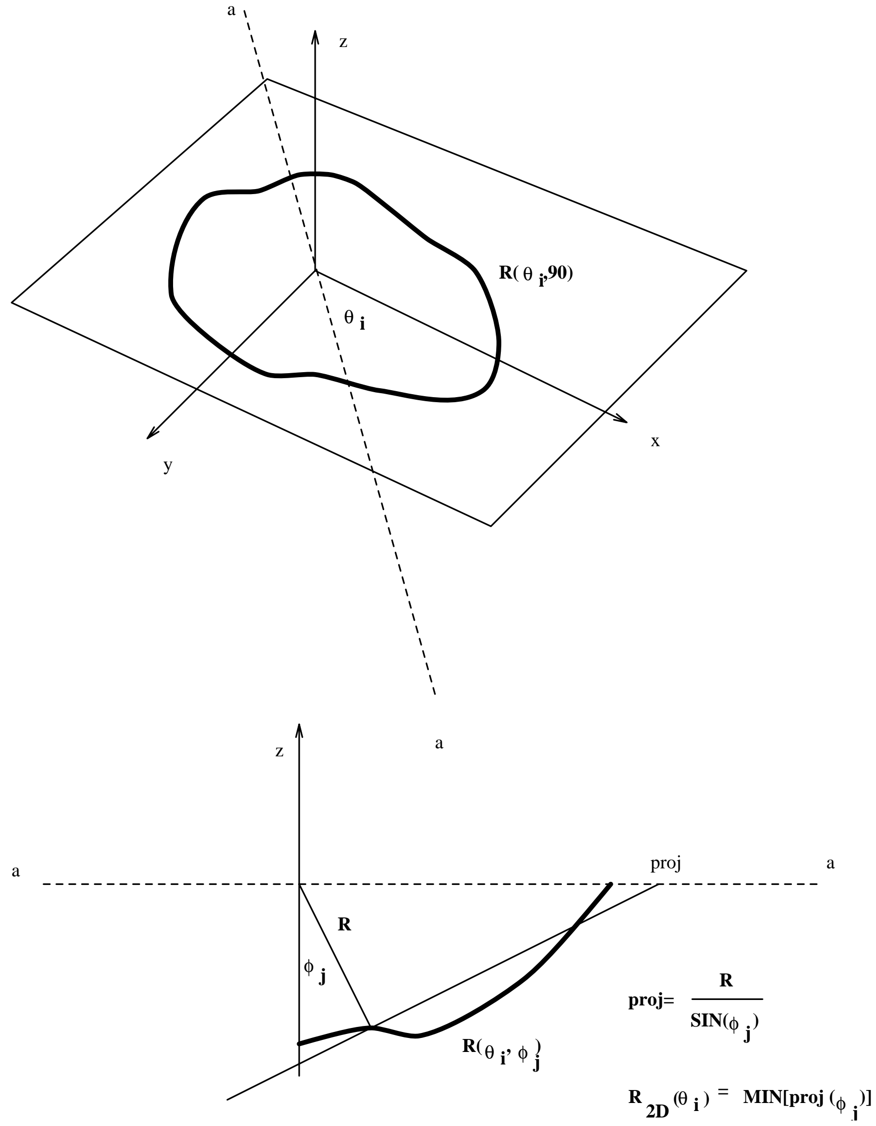

Figure 8: Minimum projection

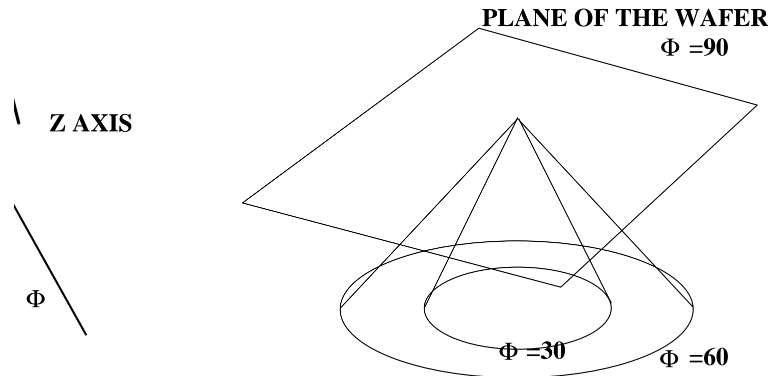

Figure 9: Projections onto cones

Generality and selection of planes

In this derivation the (111), (110), (100), and (311) rates have been chosen as principal planes. These planes were chosen because they appear quite often in the anisotropic etching of silicon. The model is in no way limited to such systems and any three principal planes may serve as a basis. Three planes is the minimum for three dimensional modeling, however more parameters improves the empirical fit of the model. While there is an infinite number of etch planes, we have found it sufficient to use the extremum planes, *i.e.* local minimum and maximum planes. If more planes are used, new triangular regions will have to be defined.

Conclusion

A method for parametrizing the full etch rate behavior given a few known rates has been presented and found to agree with experimental measurements. The model does not seek to understand the reasons why etch rates differ, but rather uses the known available data to predict the results of differing etch rates. The method clarifies both the three dimensional nature of the etch rate diagram as well as the observed etch rates for different wafer planes. The predictions of any MEMS CAD tools can only be as good as the data it is provided. A standardized system for measuring and classifying different etchant based on their etch rate behavior is a much needed aspect of MEMS design. The model outlined above can provide a valuable contribution to such a system.

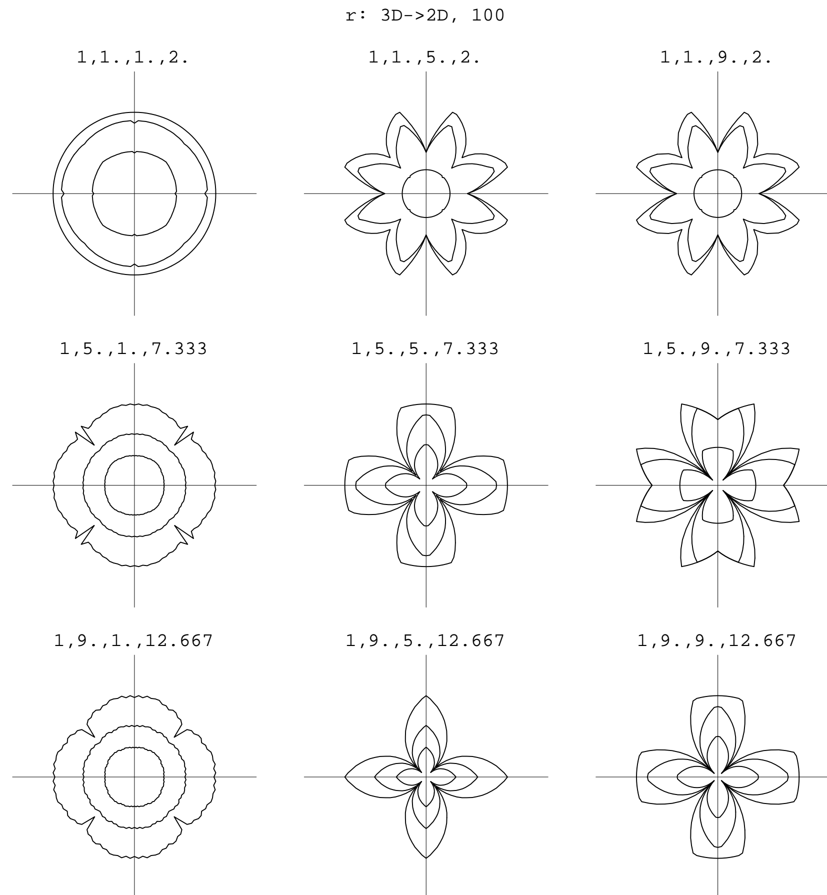

Figure 10: Modeled (100) projection, the indices *e.g.* (1,1,5,2) represent the relative weight in the basis model of (111), (110), (100), and (311) planes

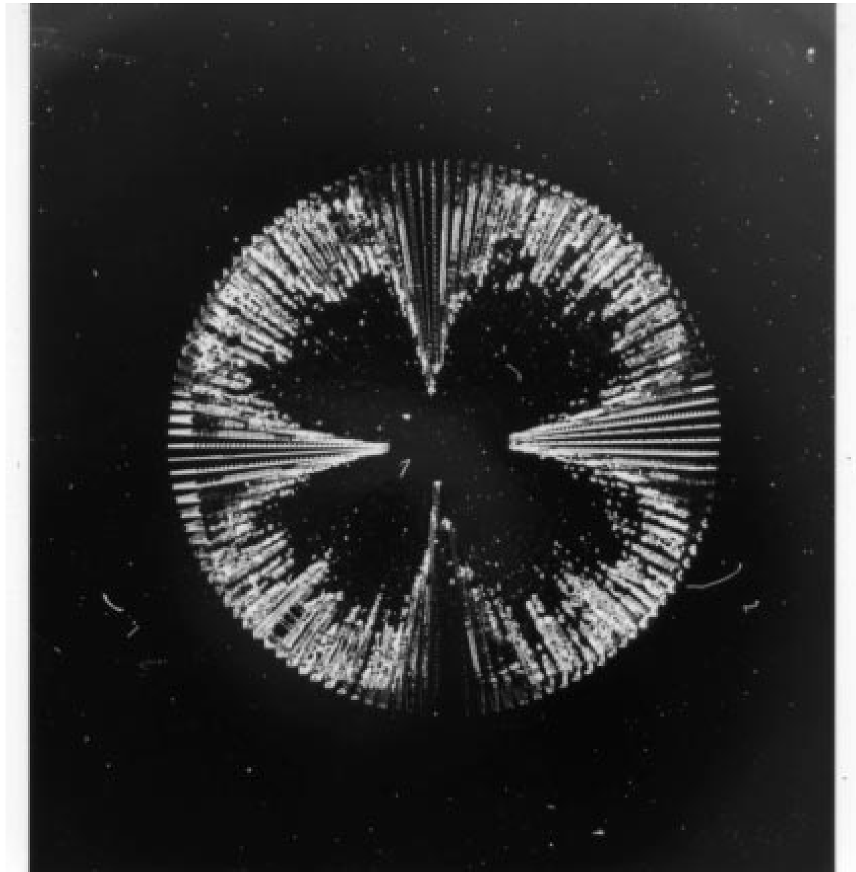

Figure 11: Experimental (100) projection, compare with Figure 10: (1,5,9,7.33)

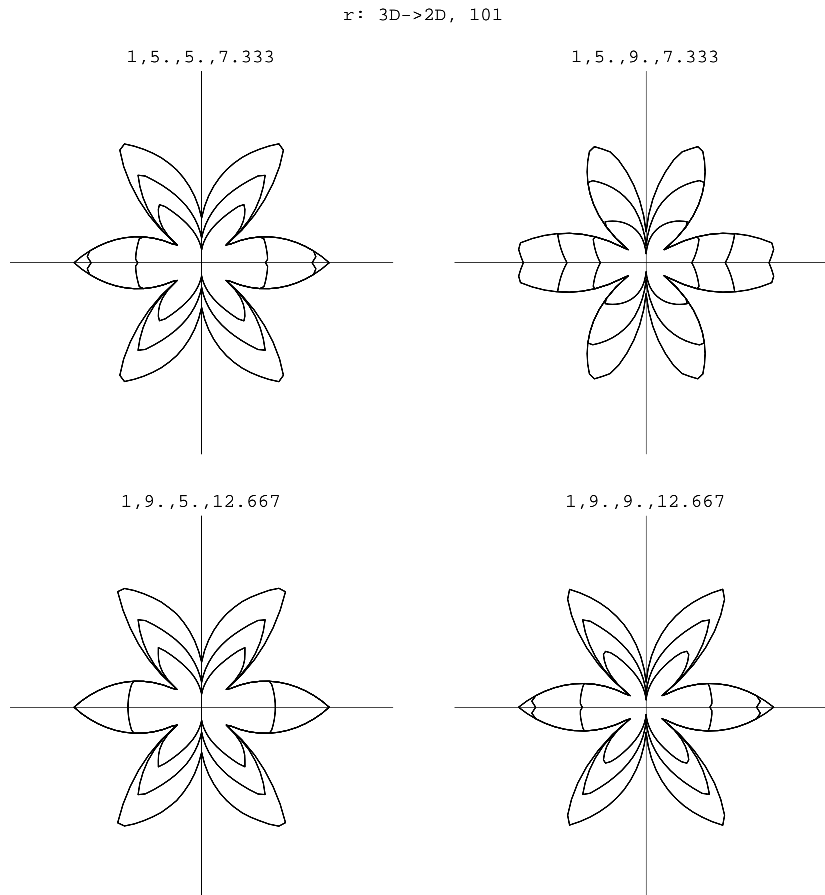

Figure 12: Modeled (110) projections, the indices *e.g.* (1,1,5,2) represent the relative weight in the basis model of (111), (110), (100), and (311) planes

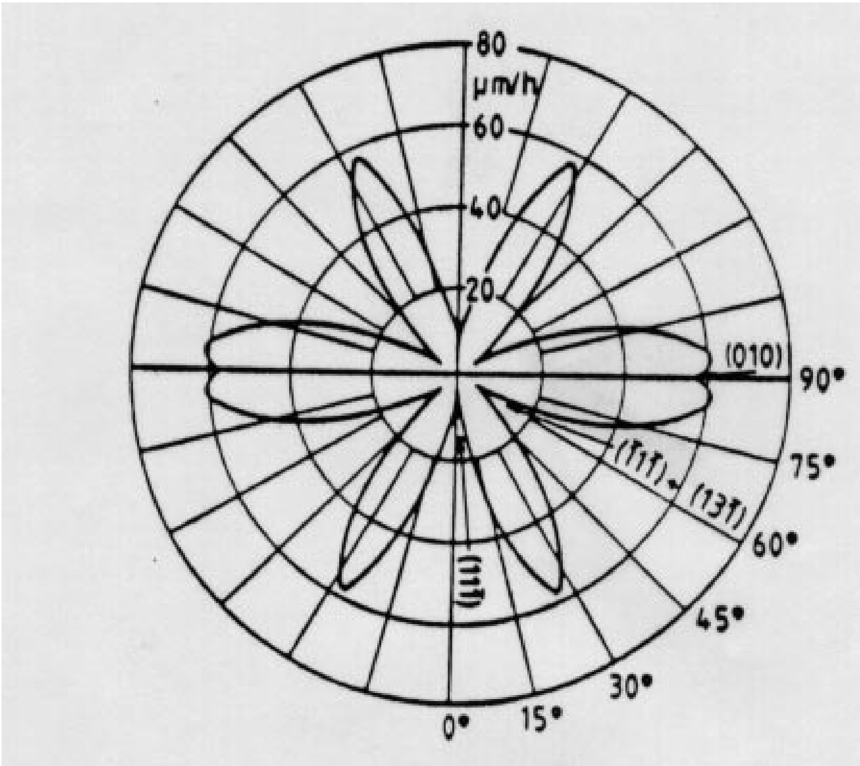

Figure 13: Experimental (110) projection from Seidel, *et al*. [9]

Acknowledgments

The authors gratefully acknowledge Professor Y.C. Tai for the use of his facilities and many helpful discussions. This material is based upon work supported, in part, by the National Science Foundation under Grant No. ECS-9023646. Any opinions, findings, conclusions or recommendations expressed in this publication are those of the authors and do not necessarily reflect the views of the sponsor.

References

[1] BUSER, R. A., AND DE ROOIJ, N. F. ASEP: A CAD program for silicon anisotropic etching. *Sensors and Actuators A-Physical 28* (1991), 71–78.

[2] DELAPIERRE, G. Anisotropic crystal etching: A simulation program. *Sensors and Actuators A-Physical 31* (1992), 267–274.

[3] HERR, E., AND BALLES, H. KOH etching of high index crystal planes in silicon. *Sensors and Actuators A-Physical 31* (1992), 283–287.

[4] HUBBARD, T. J., AND ANTONSSON, E. K. Emergent Faces in Crystal Etching. *Journal of Microelectomechanical Systems 3*, 1 (Mar. 1994), 19–28.

[5] HUBBARD, T. J., AND ANTONSSON, E. K. Design of MEMS via Efficient Simulation of Fabrication. In *Design for Manufacturing Conference* (Aug. 1996), ASME.

[6] HUBBARD, T. J., AND ANTONSSON, E. K. Cellular Automata in MEMS Design. *Sensors and Materials 9*, 7 (1997), 437–448.

[7] KOIDE, A., SATO, K., AND TANAKA, S. Simulation of two dimensional etch profile of silicon during orientation-dependent anisotropic etching. In *Transducers '91* (Institute of Electrical Engineers, 1991), pp. 216–220.

[8] SCHNAKENBERG, U., BENECKE, W., AND LOCHEL, B. NH4 OH - based etchants for silicon micromachining. *Sensors and Actuators A-Physical 21-23* (1990), 1031–1035.

[9] SEIDEL, H., CSEPREGI, L., HEUBERGER, A., AND BAUMGARTEL, H. Anisotropic etching of crystaline silicon in alkaline solutions. *J. Electrochem. Soc. 137* (1990), 3613–3631.

[10] SEQUIN, C. H. Computer simulation of anisotropic crystal etching. *Sensors and Actuators A Physical 34*, 3 (Sept. 1992), 225–241.

[11] SHAW, D. W. Morphology analysis in localized crystal growth and dissolution. *J. Cryst. Gr. 47* (1979), 509–517.

[12] THAN, O., AND BUTTGENBACH, S. Simulation of anisotropic chemical etching of crytalline silicon using a cellular-automata model. *Sensors and Actuators A-Physical 45* (1994), 85–89.

[13] THURGATE, T. Segment based etch algorithm and modeling. *IEEE Transactions on computer-aided design 10*, 9 (Sept. 1991), 1101–1109.

[14] WEIRAUCH, D. F. Correlation of the anisotropic etching of single crystal silicon spheres and wafers. *J. Appl. Phys. 46* (1975), 1478–1483.